

# Northumbria Research Link

Citation: Jamil, Muhammad Ahmad, Goraya, Talha S., Yaqoob, Haseeb, Shahzad, Muhammad Wakil and Zubair, Syed M. (2022) Experimental and Numerical Analysis of a Plate Heat Exchanger Using Variable Heat Transfer Coefficient. Heat Transfer Engineering, 43 (18). pp. 1566-1578. ISSN 0145-7632

Published by: Taylor & Francis

URL: <https://doi.org/10.1080/01457632.2021.1989841>  
<<https://doi.org/10.1080/01457632.2021.1989841>>

This version was downloaded from Northumbria Research Link:  
<https://nrl.northumbria.ac.uk/id/eprint/47864/>

Northumbria University has developed Northumbria Research Link (NRL) to enable users to access the University's research output. Copyright © and moral rights for items on NRL are retained by the individual author(s) and/or other copyright owners. Single copies of full items can be reproduced, displayed or performed, and given to third parties in any format or medium for personal research or study, educational, or not-for-profit purposes without prior permission or charge, provided the authors, title and full bibliographic details are given, as well as a hyperlink and/or URL to the original metadata page. The content must not be changed in any way. Full items must not be sold commercially in any format or medium without formal permission of the copyright holder. The full policy is available online: <http://nrl.northumbria.ac.uk/policies.html>

This document may differ from the final, published version of the research and has been made available online in accordance with publisher policies. To read and/or cite from the published version of the research, please visit the publisher's website (a subscription may be required.)

# Experimental and numerical analysis of a plate heat exchanger using variable heat transfer coefficient

Muhammad Ahmad Jamil<sup>a,b</sup>, Talha S. Goraya<sup>b</sup>, Haseeb Yaqoob<sup>b,c</sup>, Muhammad Wakil Shahzad<sup>a</sup>, and Syed M. Zubair<sup>d\*</sup>

<sup>a</sup>Mechanical & Construction Engineering Department, Northumbria University, Newcastle Upon Tyne NE1 8ST, UK

<sup>b</sup>Department of Mechanical Engineering, Khwaja Fareed University of Engineering and Information Technology, Rahim Yar Khan, Pakistan

<sup>c</sup>School of Mechanical Engineering, Universiti Sains Malaysia, Engineering Campus, Nibong Tebal, Penang, 14300, Malaysia

<sup>d</sup>Mechanical Engineering Department, KFUPM Box # 1474 King Fahd University of Petroleum & Minerals, Dhahran 31261, Saudi Arabia

## ABSTRACT

Thermal design and analysis of heat exchangers are predominantly conducted considering constant heat transfer coefficients. However, these vary along the length and affect the calculations of heat transfer rates and area allocations. The current paper investigates the variations in the heat transfer coefficients in plate heat exchangers (PHX), using different numerical approaches. The heat transfer coefficient is calculated at the inlet, outlet, and systematically selected intermediate points for each method. The analysis is conducted for two different systems, i.e., a laboratory-scale and an industrial scale PHX at different chevron angles. It is concluded that the effect of the variable heat transfer coefficient is more significant for the large-scale heat exchanger due to high flow rates, geometrical specifications, Reynolds number, and thermophysical properties. The deviation of the local heat transfer coefficient along the heat exchanger length is approximately 9-14 % and 3-6% for industrial and laboratory scale PHX, while an area deviation of around 15% is observed.

---

\* Corresponding author; e-mail: [smzubair@kfupm.edu.sa](mailto:smzubair@kfupm.edu.sa); fax # 966-13-860-2949; phone # 966-13-860-3135

Similarly, the heat transfer coefficient's variation along the heat exchanger length for ammonia, propane, ethane, and ethylene is approximately 2.1, 5.3, 5.1, and 4.9%, respectively.

## Introduction

Single-phase plate heat exchangers (PHX) offer several benefits like close temperature control, compact size, easy maintenance, and flexibility to deal with viscous fluids [1–3]. These are commonly employed to recover and utilize waste heat in power plants [4], desalination systems [5, 6], steam generation facilities [7], process [8], and refrigeration industries [9]. Therefore, a significant improvement in their thermal performance has been achieved by modifying the geometric parameters [10, 11], flow configurations [12, 13], plate material, and fouling behavior [14, 15]. The most critical geometric parameter influencing the heat transfer coefficient of PHXs is reported to be the plate chevron angle ( $\beta$ ) [16]. It is frequently said that the lower chevron angle plates offer higher heat transfer coefficients; however, the pressure drop is also higher concomitantly [17, 18]. The optimization of these geometric and flow parameters has also been adopted using different numerical techniques like dynamic modeling [19, 20], artificial neural network [21], genetic algorithm [22], and particle swarm algorithm [23, 24] which have proven to be effective in improving the heat exchanger (HX) performance.

It is essential to mention that in almost all the studies conducted hitherto, the thermal characteristics of PHXs are investigated using uniform overall heat transfer coefficients. Whereas the heat transfer coefficients vary along the heat exchanger length (flow direction) because of variations in the thermophysical properties of fluids [25, 26]. Different researchers have reported the significance of considering non-uniform heat transfer coefficients for other heat transfer systems. For instance, Balkan [27] showed that the entropy minimization achieved using the variable heat transfer coefficient produced better and precise results. Mokheimer [28] reported a significant variation in the efficiency of different fins under constant and variable heat transfer coefficients. He concluded that by involving the variable heat transfer coefficient, the deviation

occurs to 32%, 38%, 39% for the straight, spine with constant profile, and radial fin with rectangle profile respectively at dimensionless parameter  $m = 5$ . Sadri et al. [29] investigated the efficiency of a straight fin with variable heat transfer coefficient and thermal conductivity for different heat transfer modes. They reported that these two factors have a significant effect, particularly at large temperature differences. Shah and Sekulic [30] investigated the heat exchangers under variable heat transfer coefficients and showed that the Colburn method provides accurate results for the linear heat transfer coefficient. However, for the non-linear heat transfer coefficient, the most precise method is the exact numerical method. Sharqawy and Zubair [31] conducted a more comprehensive study in this regard. They presented improved analytical and numerical methods for concentric tube heat exchanger to analyze the heat transfer area variation and reported a deviation of  $\sim 17\%$  by taking a variable heat transfer coefficient. They suggested that the Chebyshev method [32] gives reasonably accurate results within a 1% deviation of the exact procedure.

The above discussion suggests that the variable heat transfer coefficient consideration in the heat exchanging systems reasonably affects the calculation of critical performance parameters (e.g., heat transfer coefficients, area, etc.). In this regard, one possibility is to use computational fluid dynamics to investigate the actual parametric distributions in the heat exchangers. Though, this approach is computationally expensive and only viable for standalone component analysis. Therefore, a more convenient and suitable option is to discretize the standard energy equations using numerical techniques.

The present study focuses on presenting a systematic procedure to examine a plate heat exchanger under variable coefficients of heat transfer that has not been conducted in literature as per the authors' knowledge. The numerical techniques used include the arithmetic mean method

(AMM), Chebyshev rule of integration (CRI), Simpson's methods (SM), and an exact numerical method (ENM), the details of which are presented in the subsequent sections. In each technique, the values of thermodynamic properties (temperature, density, viscosity, conductivity, etc.) and the corresponding Reynolds number ( $Re$ ), Nusselt number ( $Nu$ ), Prandtl number ( $Pr$ ), and the heat transfer coefficients ( $h_c$ ,  $h_h$ ,  $U$ ) are calculated at the inlet, outlet and systematically selected intermediate points. Finally, the average heat transfer coefficient is calculated as an arithmetic mean of all the values. By using the average heat transfer coefficients from each procedure, the corresponding heat transfer area is determined. The values are compared with the constant heat transfer coefficient case, and the percentage deviation in the heat transfer coefficient and the area is estimated.

## Materials and methods

### Thermal design

A conventional plate heat exchanger used for ordinary heating/cooling purposes is considered in the current study. Engineering equation solver (EES) based numerical code for the calculated local, total heat transfer coefficient, heat duty, and heat transfer area is created by using the governing equation (see Appendix Table A-1 [33–35]). The local heat transfer coefficient is calculated as a function of  $Nu$ ,  $Re$ ,  $Pr$ , and  $(\beta)$ , as given in Eq. (1) [36–38].

$$Nu = C_h \times Re^{n'} \times Pr^{\frac{1}{3}} \times \left( \frac{\mu}{\mu_w} \right)^{0.14} \quad (1)$$

where  $C_h$  and  $n'$  vary with  $Re$  and  $\beta$  as given in Appendix A, Table A-2 [33–36, 39].

## Experimental arrangement

The laboratory-scale PHX (Model: edibon-TIPL-0083/16) is used for experimental validation. The PHX consists of a base unit for regulating the hot stream flow rates and temperature while supplying the cold water via an external hydraulic bench (Model: FM-1849). Figure 1 illustrates a schematic of the experimental setup, while the geometry with all appropriate dimensions and the internals are presented in Figure 2. The design parameters for the testing and industry-scale plate heat exchangers are shown in Table 1.

## Numerical approaches for variable heat transfer coefficient

For a given PHX, the energy balance is given as.

$$d\dot{Q} = -\dot{C}_h dT_h = -\dot{C}_c dT_c = dU(A\Delta T) \quad (2)$$

where the heat duty is represented by  $\dot{Q}$ , and  $\Delta T = T_h - T_c$  is the temperature difference between the hot and cold fluid. Eq. (2) is integrated to calculate the overall heat transfer coefficient.

$$U = \int_{T_{h,i}}^{T_{h,o}} \frac{-\dot{C}_h dT_h}{A\Delta T} = \int_{T_{c,i}}^{T_{c,o}} \frac{-\dot{C}_c dT_c}{A\Delta T} \quad (3)$$

Different numerical approaches are used to solve the above equation. Equation (3) can be discretized for the hot- and cold-fluid as

$$U = \int_{T_{h,i}}^{T_{h,o}} \frac{-\dot{C}_h dT_h}{A\Delta T} \approx \frac{\dot{m}_h(T_{h,o} - T_{h,i})}{k} \left[ \sum_{x_i}^{x_n} \left( \frac{c_{p,h}}{A\Delta T} \right) \right] \quad (4)$$

$$U = \int_{T_{c,i}}^{T_{c,o}} \frac{-\dot{C}_c dT_c}{A\Delta T} \approx \frac{\dot{m}_c(T_{c,o} - T_{c,i})}{k} \left[ \sum_{x_i}^{x_n} \left( \frac{c_{p,c}}{A\Delta T} \right) \right] \quad (5)$$

where  $k$ ,  $x_i$ , and  $x_n$  are the number of selected points, initial point, and final point, respectively. In Eq. (6), the temperature difference and thermophysical properties are dependent upon the intermediate temperature points located by different numerical approaches. The middle-point temperature is calculated as

$$T_{h(x)} = T_{h,i} - x \Delta T_h \quad (6)$$

$$T_{c(x)} = T_{c,i} + x \Delta T_c \quad (7)$$

The  $x$  refers to the location of the intermediate temperature point over the length of the heat exchanger.

After calculating thermophysical properties at intermediate points, the hot and cold side's local heat transfer coefficient is determined at selected points, which further combines using Eq. (8) to get the overall heat transfer coefficient.

$$\frac{1}{U} = \frac{1}{h_h} + \frac{1}{h_c} + \frac{t}{k'} + R_{f,h} + R_{f,c} \quad (8)$$

### **Arithmetic mean method**

In heat exchanger study, this approach is widely used and serves as a base case for the current work. The cold and hot fluid's thermophysical properties are calculated at their respective mean values of inlet and outlet. The hot and cold fluid temperature at specified points can be calculated from the equations in the subsection. After calculating temperatures and thermophysical properties at the inlet ( $x_i$ ) and outlet ( $x_n$ ) point, the local, overall heat transfer coefficient, and area of HX can be calculated. A detailed discussion of this numerical approach can be found in the heat exchanger textbook [40, 41].



## Chebyshev integration method

It is also known as a four-point integration method and works by calculating the required quantity at four intermediate points in addition to inlets and outlets. These points are taken at 10%, 40%, 60%, and 90% of the respective fluid's absolute temperature difference. The temperature depends on the thermophysical properties of hot and cold fluids are calculated at their selected points which are further utilized to calculate the local overall heat transfer coefficient. Sharqawy and Zubair [31] have discussed the comprehensive formulation, including the four-point integration method for HX.

## Simpson's (n = 2, 4 and 8) methods

The method offers flexibility to vary the intermittent points, thus facilitating the integration of complex formulations. In this paper, Simpson's rule is used; the number of segments is the multiple of 2 such as (n=2,4 and 8). The temperature and thermophysical properties are calculated at each point to study the variation in the local heat transfer coefficient. Simpson's (n=2) method is the simplest case that uses inlet and outlet boundary conditions with the addition of a mid-point. This method provides a more precise and accurate result by adding the intermediate point between the inlet and outlet boundary. Therefore, the method is modified by increasing the number of segments as n=4 and 8, which uses five and nine intermediate points, respectively [40].

## Exact numerical method

The exact numerical (n=100) method approach is an effective technique to solve integration. In the current case, the heat exchanger is fractionated into a hundred intermediate points at which the properties are calculated at the selected points, and variation of the local heat transfer

coefficient is examined. This approach utilizes an extensive number of intermediate points for an accurate estimation.

It is essential to mention that all the above-discussed numerical techniques work on the same principle of discretizing the energy equation. It is important to note that the number of nodes at which temperature, thermophysical properties, Reynolds number, Prandtl number, and heat transfer coefficients are calculated to differ depending upon the technique. A detailed graphical representation and the corresponding numerical formulation consisting of intermediate point selection and boundary conditions for comparison are summarized in [Table 2](#). It emphasizes that the selection of nodes and parameters is well defined in the technique's mathematical development and is only utilized in the current study.

## **Numerical solution and assumption**

An EES-based numerical code is generated using the above-mentioned governing equations. The numerical code is first validated with the experimental setup. After that, the temperatures and thermophysical properties are calculated at the intermediate [points](#) generated by the numerical approaches. It is followed by calculating Reynolds number, Nusselt number, effective area, local-and-overall variable heat transfer coefficient. A laboratory and full-scale plate heat exchanger are then investigated to examine the local heat transfer coefficient variation. The solution flow chart is represented in Figure 3. This study is based on the following assumptions: (a) variable heat transfer coefficients, (b) steady-state process, (c) negligible longitudinal heat conduction, (d) minor thermal and hydraulic losses in connecting pipes, (e) the system-wide incompressible fluid flow, and (f) the hot fluid dissipated the cold fluid fully absorbs heat.

## Results and discussion

### Experimental validation

The EES numerical code is developed and validated with the experimental data from a laboratory-scale PHX (Model: edibon-TIPL-0083/16) as illustrated in Figure 1. The experimental setup's geometric specifications are summarized in Table 1, and the corresponding internal details of the heat exchanger plate are presented in Figure 2. The experiments were conducted for ten different sets of variables; each run was operated for 35 minutes; the details are shown in Table 3. The data was recorded in the data acquisition system (edibon-SCADA) and imported into EES software by using the look-up table command. Then the numerical results were validated with the experimental data, which showed a very close agreement between each other, as shown in Figure 4. However, the error deviation between the numerical and experimental values was calculated to be within  $\pm 5\%$  due to the instruments' inaccuracy and non-negligible heat losses.

After validation at various operating conditions, the uncertainty propagation analysis was conducted to estimate the total uncertainty in the calculated parameters, i.e., the overall heat transfer coefficient,  $U$  due to the instruments' inaccuracy. The input parameters are modeled as a sum of their nominal value ( $\bar{X}$ ) and uncertainty ( $U'_X$ ), as given below [42].

$$X = \bar{X} \pm U'_X \quad (9)$$

The corresponding uncertainty in the response variable  $Y$  due to  $U'_X$  is calculated as [43],

$$U'_Y = \frac{dY}{dX} U'_X \quad (10)$$

The total uncertainty in Y due to X's variations is given by the root sum square product of the individual uncertainties computed to the first-order accuracy for a multi-variate function  $Y = Y(X_1, X_2, \dots, X_N)$  as [39].

$$U'_Y = \left[ \sum_{i=1}^N \left( \frac{\partial Y}{\partial X_i} U'_{X_i} \right)^2 \right]^{1/2}$$

$$= \left\{ \left( \frac{\partial Y}{\partial X_1} U'_{X_1} \right)^2 + \left( \frac{\partial Y}{\partial X_2} U'_{X_2} \right)^2 + \dots + \left( \frac{\partial Y}{\partial X_N} U'_{X_N} \right)^2 \right\}^{1/2} \quad (11)$$

The accuracy of temperature sensors was taken  $\pm 0.5^\circ\text{C}$  and flow sensors are  $\pm 1\%$  in the current analysis. The analysis showed that the uncertainty in overall heat transfer coefficient due to  $T_c$  was  $\pm 0.1984$ ,  $T_h$  as  $\pm 0.1695$ ,  $V_c$  as  $\pm 0.8905$ , and  $V_h$  as  $\pm 0.8187$ . Therefore, the total uncertainty is calculated as the root sum square product of the individual variations to the first-order accuracy in U was  $\pm 1.265$ .

## Laboratory scale PHX

After the validation, the laboratory-scale plate heat exchanger was run to examine the variable heat transfer coefficient variation. In the current study, the hot side was selected to visualize the variation of heat transfer because, in PHX, both sides are identical but opposite in trend. The variation of local heat transfer coefficient by different numerical approaches is illustrated in Figures 5 (a) to (f). From Figure 5, it can be observed that the deviation was slight on a laboratory scale due to the small mass flow rate and geometry specification. For example, the variation of local heat transfer coefficient was  $\pm 6\%$  for chevron angle  $\beta$

$$\beta$$

for chevron angles  $\beta = 60^\circ$  and  $65^\circ$  is not presented because, at a high chevron angle, the effect of variable heat transfer coefficient was minor due to less enhancement of Reynolds number.

Furthermore, for the chevron angle  $\beta = 30^\circ$ , the values of uniform and average heat transfer coefficient by all numerical approaches were observed to be very close (i.e.,  $\pm 1\%$ ); thus, exhibits that the effects on the thermal performance of heat exchanger are marginal for small scale HX.

## Industrial-scale PHX

After laboratory-scale, an industrial-scale HX was considered to investigate the heat transfer coefficient's variation at high flow rates, temperature differences, and heat duty. It can be explained that the effect of different parameters dilutes or intensifies at different heat exchanger sizes. For example, the impact of end plates on PHX performance reduces at a higher number of plates and becomes significant when there are fewer plates. The effect of the variable local heat transfer coefficient by different numerical approaches is illustrated in Figures 6 (a) to (f). It was observed that the variation in heat transfer coefficient was significant in the industrial-scale heat exchanger (refer to Figure 6) compared to the laboratory-scale heat exchanger (refer to Figure 5). This is because of having high process specification, geometric parameters, and thermophysical properties. For example, the deviation of the local heat transfer coefficient along the heat exchanger was within the range of  $\sim 9\text{-}14\%$  for different chevron angles, as shown in Figs. 5 (a) to (f). Furthermore, for the chevron angle  $\beta = 30^\circ$ , the values of uniform and average heat transfer coefficient by all numerical approaches revealed a markable deviation due to the local heat transfer coefficient having  $9\text{-}14\%$  deviation along the length of large scale HX. It indicates that special attention is needed towards the variable heat transfer coefficient approach in designing for such a large-scale component.

## Deviation in the heat transfer area

Based on the variation in local heat transfer coefficients as presented above, the overall heat transfer coefficient was calculated as  $\sim 3\text{-}6\%$  and  $\sim 9\text{-}14\%$  for laboratory scale and industrial scale PHXs, respectively. The corresponding area deviations for different numerical approaches for the industrial-scale plate heat exchanger are presented in Table 4. The area deviation ( $\leq \pm 15\%$ ) was observed, which affects the heat exchanger's capital investment. Therefore, attention is required, especially for large-scale heat exchangers, on the variable heat transfer coefficient for accurate thermal and economic performance prediction.

## Heat transfer coefficient for different fluids

After a detailed investigation of deviation in the laboratory and industrial-scale heat exchanger for water, the study was extended to different fluids to examine the heat transfer coefficient's varying behavior. For this investigation, the fluids selected included ammonia, propane, ethane, and ethylene in a PHX with  $\beta = 30^\circ$ . The variation in heat transfer coefficient is presented in Figure 7, which shows about  $\pm 2.1\%$ ,  $\pm 5.3\%$ ,  $\pm 5.1\%$ , and  $\pm 4.9\%$  deviation for ammonia, propane, ethane, and ethylene, respectively if we compared the intermediate points 0.1 and 0.9 along the heat exchanger length. It implies that the fluids with high thermophysical properties dependent on temperature will observe large variations in the heat transfer coefficient along the heat exchanger length.

## Concluding remarks

The current study presents a systematic procedure for the analysis of PHX under the variable heat transfer coefficient. For this purpose, an experimentally validated EES-based numerical code was employed to study the heat transfer coefficient variation along the heat exchanger length for laboratory and industrial-scale PHXs. The different numerical approaches used to discretize the energy balance equation included AMM, CRI, SM, and ENM. The study verified that the heat transfer coefficient was not uniform. Instead, it varied along the heat exchanger length. It decreased for the hot side and increased for the cold side from the inlet to the fluid outlet. The significant findings of the study under current operating scenarios are summarized below:

- The local heat transfer coefficient variation was dominant for large/industrial heat exchangers with  $\sim 9\text{-}14\%$  compared to the small/laboratory scale HX having  $\sim 3\text{-}6\%$  for different numerical approaches.
- The variation in local heat transfer coefficients along the heat exchanger length for different fluids, i.e., ammonia, propane, ethane, and ethylene, was observed to be of the order of  $\pm 2.1\%$ ,  $\pm 5.3\%$ ,  $\pm 5.1\%$ , and  $\pm 4.9\%$ , respectively.
- The heat transfer area deviation calculated using variable heat transfer coefficient approaches is observed as  $\leq \pm 15\%$  compared to the constant heat exchanger area.
- Among different numerical approaches used, the CRI (which employed only four intermediate points) is recommended to analyze the heat exchangers. It produced results reasonably close to the exact numerical method with many discretizing points (i.e., 100 in the current study).

## Acknowledgments

The authors acknowledge the support provided by Northumbria University, UK under reference# RDF20/EE/MCE/SHAHZAD. Also, acknowledge the support provided by Engr. Shahzeen Syed (an undergraduate student at KFUEIT) for graphical work presented in Table 2.

## Nomenclature

$A$	area of heat transfer, $m^2$
$A_l$	area of single plate heat transfer, $m^2$
$A_{lp}$	area of the projected plate, $m^2$
$A_c$	cross-section area used in Table A-1
AMM	arithmetic mean method
$b$	mean gap of channel flow, m
$C_h$	Nusselt number constant for measurement in Table A-2
$c_p$	specific heat, $kJ/kg \cdot K$
$\dot{C}$	parameter in Eq. (2), $kJ/K \cdot s$
CF	cleanliness factor
CRI	Chebyshev rule of integration
$D_p$	diameter of port, m
$D_h$	hydraulic diameter, m
EES	engineering equation solver
ENM	exact numerical method
$G$	mass velocity, $kg/m^2 \cdot s$
$h$	heat transfer coefficient, $W/m^2 \cdot K$



HX	heat exchanger
$k'$	thermal conductivity, W/m·K
$k$	number of selected intermediates point
$K_p$	pressure drop constant for measurement in Table A-2
$L_c$	compressed plate pack length, m
$L_h$	distance of horizontal port, m
$L_p$	projected plate length, m
$L_v$	distance of vertical port, m
$L_w$	width of effective channel, m
LMTD	log mean temperature difference
$\dot{m}$	mass flow rate, kg/s
$N_{cp}$	number of channels/pass
$N_e$	the effective number of plates
$N_P$	passes number
$N_t$	plates number
$Nu$	Nusselt number
$n$	segments/parts
OS	over surface design
$P$	pressure in Figure 3
$p'$	pitch in Table A-1, mm
$P_w$	perimeter in Table A-1, mm
$Pr$	Prandtl number
PHX	plate heat exchanger

$\dot{Q}$	heat duty, kW
$R_f$	fouling resistance, $\text{m}^2 \cdot \text{K} / \text{W}$
$Re$	Reynolds number
SM's	Simpson's methods
SS	stainless steel
t	plate thickness in Eq. (8) & Table A-1
$\Delta T$	temperature difference
T	temperature, $^{\circ}\text{C}$
$U$	overall heat transfer coefficient, $\text{W}/\text{m}^2 \cdot \text{K}$
$U'_X$	uncertainty in X variable
$U'_Y$	uncertainty in Y variable
V	volume flow rate, liter/min
X	variable in Eq. (9)
$\bar{X}$	nominal value
x	location of the intermediate point, mm
Y	variable in Eq. (10)

### Greek Symbols

$\beta$	chevron angle, deg
$\phi$	enlargement factor
$\rho$	density, $\text{kg}/\text{m}^3$
$\mu$	dynamic viscosity, $\text{kg}/\text{m} \cdot \text{s}$
$\Delta T$	change in temperature, $^{\circ}\text{C}$

$\Delta T_{\text{LMTD}}$	log mean temperature difference, °C
$\Delta x$	increment in intermediate points, mm

### Subscripts

$c$	cold
$ch$	per channel
$c,i$	cold inlet
$cl$	clean
$c,o$	cold outlet
$e$	effective
$f$	fouling/fouled
$h$	hot
$h,i$	hot inlet
$h,o$	hot outlet
$i$	initial point
$n$	final point
$p$	port
$\text{tot}$	total
$w$	wall

### Superscripts

$m$	pressure drop number constant for measurement in Table A-2
$n'$	Nusselt number constant for measurement in Table A-2

## References

- [1] T. S. Khan, M. S. Khan, and Z. H. Ayub, "Single-Phase Flow Pressure Drop Analysis in a Plate Heat Exchanger," *Heat Transf. Eng.*, vol. 38, no. 2, pp. 256–264, April 2016. <https://doi.org/10.1080/01457632.2016.1177430>.
- [2] J. A. W. Gut and J. M. Pinto, "Modeling of plate heat exchangers with generalized configurations," *Int. J. Heat Mass Transf.*, vol. 46, no. 14, pp. 2571–2585, January 2003. [https://doi.org/10.1016/S0017-9310\(03\)00040-1](https://doi.org/10.1016/S0017-9310(03)00040-1).
- [3] B. Palm and J. Claesson, "Plate heat exchangers: Calculation methods for single and two-phase flow," *Heat Transf. Eng.*, vol. 27, no. 4, pp. 88–98, August 2006. <https://doi.org/10.1080/01457630500523949>.
- [4] H. Mergner and K. Schaber, "Performance analysis of an evaporation process of plate heat exchangers installed in a Kalina power plant," *Energy*, vol. 145, pp. 105–115, December 2017. <https://doi.org/10.1016/j.energy.2017.12.105>.
- [5] E. Yang, K. J. Chae, M. J. Choi, Z. He, and I. S. Kim, "Critical review of bioelectrochemical systems integrated with membrane-based technologies for desalination, energy self-sufficiency, and high-efficiency water and wastewater treatment," *Desalination*, vol. 452, pp. 40–67, October 2018. <https://doi.org/10.1016/j.desal.2018.11.007>.
- [6] M. A. Jamil and S. M. Zubair, "Design and analysis of a forward feed multi-effect mechanical vapor compression desalination system: An exergo-economic approach," *Energy*, vol. 140, pp. 1107–1120, August 2017. <https://doi.org/10.1016/j.energy.2017.08.053>.
- [7] J. Yu and H. Zhao, "A numerical model for thermoelectric generator with the parallel-plate heat exchanger," *J. Power Sources*, vol. 172, no. 1, pp. 428–434, July 2007. <https://doi.org/10.1016/j.jpowsour.2007.07.045>.
- [8] P. Rašković, A. Anastasovski, L. Markovska, and V. Meško, "Process integration in bioprocess industry: waste heat recovery in yeast and ethyl alcohol plant," *Energy*, vol. 35, no. 2, pp. 704–717, December 2009. <https://doi.org/10.1016/j.energy.2009.11.020>.
- [9] Z. H. Ayub, "Plate heat exchanger literature survey and new heat transfer and pressure drop

- correlations for refrigerant evaporators,” *Heat Transf. Eng.*, vol. 24, no. 5, pp. 3–16, November 2010. <https://doi.org/10.1080/01457630304056>.
- [10] A. Durmuş, H. Benli, I. Kurtbaş, and H. Gül, “Investigation of heat transfer and pressure drop in plate heat exchangers having different surface profiles,” *Int. J. Heat Mass Transf.*, vol. 52, no. 5–6, pp. 1451–1457, October 2008. <https://doi.org/10.1016/j.ijheatmasstransfer.2008.07.052>.
- [11] C. Gulenoglu, F. Akturk, S. Aradag, N. Sezer Uzol, and S. Kakac, “Experimental comparison of performances of three different plates for gasketed plate heat exchangers,” *Int. J. Therm. Sci.*, vol. 75, pp. 249–256, July 2013. <https://doi.org/10.1016/j.ijthermalsci.2013.06.012>.
- [12] A. Lozano, F. Barreras, N. Fueyo, and S. Santodomingo, “The flow in an oil/water plate heat exchanger for the automotive industry,” *Appl. Therm. Eng.*, vol. 28, pp. 1109–1117, September 2007. <https://doi.org/10.1016/j.applthermaleng.2007.08.015>.
- [13] K. Sarraf, S. Launay, and L. Tadrist, “Complex 3D-flow analysis and corrugation angle effect in plate heat exchangers,” *Int. J. Therm. Sci.*, vol. 94, pp. 126–138, March 2015. <https://doi.org/10.1016/j.ijthermalsci.2015.03.002>.
- [14] H. U. Zettler, M. Weiß, Q. Zhao, and H. Müller-Steinhagen, “Influence of surface properties and characteristics on fouling in plate heat exchangers,” *Heat Transf. Eng.*, vol. 26, no. 2, pp. 3–17, February 2005. <https://doi.org/10.1080/01457630590897024>.
- [15] B. Thonon, S. Grandgeorge, and C. Jallut, “Effect of geometry and flow conditions on particulate fouling in plate heat exchangers,” *Heat Transf. Eng.*, vol. 20, no. 3, pp. 12–24, October 2010. <https://doi.org/10.1080/014576399271385>.
- [16] B. Kumar, A. Soni, and S. N. Singh, “Effect of geometrical parameters on the performance of chevron type plate heat exchanger,” *Exp. Therm. Fluid Sci.*, vol. 91, pp. 126–133, September 2017. <https://doi.org/10.1016/j.expthermflusci.2017.09.023>.
- [17] H. Hajabdollahi, M. Naderi, and S. Adimi, “A comparative study on the shell and tube and gasket-plate heat exchangers: The economic viewpoint,” *Appl. Therm. Eng.*, vol. 92, pp. 271–282, August 2015. <https://doi.org/10.1016/j.applthermaleng.2015.08.110>.

- [18] K. Nilpueng, T. Keawkamrop, H. S. Ahn, and S. Wongwises, "Effect of chevron angle and surface roughness on thermal performance of single-phase water flow inside a plate heat exchanger," *Int. Commun. Heat Mass Transf.*, vol. 91, pp. 201–209, February 2018. <https://doi.org/10.1016/j.icheatmasstransfer.2017.12.009>.
- [19] Y. Wang et al., "State-space model and robust control of plate heat exchanger for dynamic performance improvement," *Appl. Therm. Eng.*, vol. 128, pp. 1588–1604, February 2018. <https://doi.org/10.1016/j.applthermaleng.2017.09.120>.
- [20] J. E. Hey, S. L. Hodson, K. Yazawa, J. Doty, and T. S. Fisher, "Experimental characterization of dynamic heat exchanger behavior," *Int. J. Heat Mass Transf.*, vol. 121, pp. 933–942, December 2017. <https://doi.org/10.1016/j.ijheatmasstransfer.2017.12.135>.
- [21] C. Turk, S. Aradag, and S. Kakac, "Experimental analysis of a mixed-plate gasketed plate heat exchanger and artificial neural net estimations of the performance as an alternative to classical correlations," *Int. J. Therm. Sci.*, vol. 109, pp. 263–269, June 2016. <https://doi.org/10.1016/j.ijthermalsci.2016.06.016>.
- [22] M. A. Jamil et al., "Optimizing the energy recovery section in thermal desalination systems for improved thermodynamic, economic, and environmental performance," *Int. Commun. Heat Mass Transf.*, vol. 124, p. 105244, March 2021. <https://doi.org/10.1016/j.icheatmasstransfer.2021.105244>.
- [23] Y. Zhang, H. Zhang, W. Zheng, S. You, and Y. Wang, "Numerical investigation of a humidification-dehumidification desalination system driven by heat pump," *Energy Convers. Manag.*, vol. 180, pp. 641–653, August 2018. <https://doi.org/10.1016/j.enconman.2018.11.018>.
- [24] Y. Zhang, H. Zhang, W. Zheng, S. You, and Y. Wang, "Optimal operating conditions of a hybrid humidification-dehumidification and heat pump desalination system with multi-objective particle swarm algorithm," *Desalination*, vol. 468, no. July, p. 114076, July 2019. <https://doi.org/10.1016/j.desal.2019.114076>.
- [25] R. Das and K. T. Ooi, "Application of simulated annealing in a rectangular fin with variable heat transfer coefficient," *Inverse Probl. Sci. Eng.*, vol. 21, no. 8, pp. 1352–1367, January

2013. <https://doi.org/10.1080/17415977.2013.764294>.
- [26] W. Roetzel and X. Luo, “Mean overall heat transfer coefficient in heat exchangers allowing for temperature-dependent fluid properties,” *Heat Transf. Eng.*, vol. 32, no. 2, pp. 141–150, October 2011. <https://doi.org/10.1080/01457631003769278>.
- [27] F. Balkan, “Application of EoEP principle with variable heat transfer coefficient in minimizing entropy production in heat exchanges,” *Energy Convers. Manag.*, vol. 46, no. 13–14, pp. 2134–2144, December 2004. <https://doi.org/10.1016/j.enconman.2004.10.020>.
- [28] E. M. A. Mokheimer, “Heat transfer from extended surfaces subject to variable heat transfer coefficient,” *Heat Mass Transf. und Stoffuebertragung*, vol. 39, no. 2, pp. 131–138, September 2002. <https://doi.org/10.1007/s00231-002-0338-3>.
- [29] S. Sadri, M. R. Raveshi, and S. Amiri, “Efficiency analysis of straight fin with variable heat transfer coefficient and thermal conductivity,” *J. Mech. Sci. Technol.*, vol. 26, no. 4, pp. 1283–1290, November 2011. <https://doi.org/10.1007/s12206-012-0202-4>.
- [30] R. K. Shah and D. P. Sekulic, “Nonuniform Overall Heat Transfer Coefficients in Conventional Heat Exchanger Design Theory — Revisited,” vol. 120, pp 520-525, May 1998. <https://doi.org/10.1115/1.2824281>.
- [31] M. H. Sharqawy and S. M. Zubair, “Heat exchangers design under variable overall heat transfer coefficient: improved analytical and numerical approaches,” *Heat Transf. Eng.*, vol. 31, no. 13, pp. 1051–1056, February 2010. <https://doi.org/10.1080/01457631003640313>.
- [32] “British Standard Water cooling towers Part 2. Methods for performance testing,” vol. 3, 1988. <http://www.iso-iran.ir/standards/bs/BS%204485%20Part%202-1988.pdf>.
- [33] A. K. Tiwari, P. Ghosh, and J. Sarkar, “Performance comparison of the plate heat exchanger using different nanofluids,” *Exp. Therm. Fluid Sci.*, vol. 49, pp. 141–151, May 2013. <https://doi.org/10.1016/j.expthermflusci.2013.04.012>.
- [34] B. D. Raja, R. L. Jhala, and V. Patel, “Thermal-hydraulic optimization of plate heat exchanger: A multi-objective approach,” *Int. J. Therm. Sci.*, vol. 124, pp. 522–535, May 2017. <https://doi.org/10.1016/j.ijthermalsci.2017.10.035>.

- [35] S. Kakac and H. Liu, *Heat Exchangers: Selection, Rating, and Thermal Design*, 2nd ed. New York: CRC, 2002.
- [36] H. Kumar, “The plate heat exchanger: construction and design, 1st UK National Conference on Heat Transfer, University of Leeds,” in *Inst. Chemical Symposium*, pp. 1275–1286, 3-5 July 1984.
- [37] W. L. Wilkinson, “Flow distribution in plate heat exchangers,” *Chem. Eng.*, vol. 285, pp. 289–292, Jan 1974.
- [38] J. Marriott, “Where and how to use plate heat exchangers,” *Chem. Eng.*, vol. 78, no. 8, p. 127, Jan 1971.
- [39] M. Ahmad, Z. Ud, T. S. Goraya, H. Yaqoob, and S. M. Zubair, “Thermal-hydraulic characteristics of gasketed plate heat exchangers as a preheater for thermal desalination systems,” *Energy Convers. Manag.*, vol. 205, p. 112425, December 2019.
- [40] R. K. Shah and D. P. Sekuli, *Fundamental of heat exchanger design*. John Wiley & Sons, Hoboken, NJ, USA, 2003. <https://doi.org/10.1002/9780470172605.ch10>.
- [41] E. U. Schlunder, *Heat Exchanger Design Handbook*, Hemisphere Publishing Corporation, Washington, DC, 1989.
- [42] I. S. Hussaini, S. M. Zubair, and M. A. Antar, “Area allocation in multi-zone feedwater heaters,” *Energy Convers. Manag.*, vol. 48, no. 2, pp. 568–575, February 2007. <https://doi.org/10.1016/j.enconman.2006.06.003>.
- [43] J. H. Kim and T. W. Simon, “Journal of heat transfer policy on reporting uncertainties in experimental measurements and results,” *J. Heat Transfer*, vol. 115, no. 1, pp. 5–6, February 1993. <https://doi.org/10.1115/1.2910670>.



## Appendix A

**Table A- 1**

Thermal design equations of PHXs.

Parameter	Relation
Reynolds number	$Re = \frac{G_{ch} D_h}{\mu}$
Mass velocity per channel (kg/m <sup>2</sup> s)	$G_{ch} = \frac{\dot{m}}{N_{cp} A_{ch}}$
Number of channels per pass	$N_{cp} = \frac{N_t - 1}{2N_p}$
Single-channel flow area (m <sup>2</sup> )	$A_{ch} = L_w \times b$
Mean gap of channel flow	$b = p' - t$
Plate pitch (m)	$p' = \frac{L_c}{N_t}$
Hydraulic diameter (m)	$D_h = \frac{4A_c}{P_w} = \frac{2b}{\phi}$
Projected plate area (m <sup>2</sup> )	$A_{l,p} = (L_v - D_p)L_w$
Enlargement factor	$A_1 = \phi A_{l,p}$
Effective heat transfer area (m <sup>2</sup> )	$A_e = A_1 N_e$
Number of effective plates	$N_e = N_t - 2$
Heat transfer coefficient (kW/m <sup>2</sup> K)	$h = \frac{Nu k'}{D_h}$
Overall clean heat transfer coefficient (kW/m <sup>2</sup> K)	$\frac{1}{U_{cl}} = \frac{1}{h_c} + \frac{t}{k'} + \frac{1}{h_h}$
Overall fouled heat transfer coefficient (kW/m <sup>2</sup> K)	$\frac{1}{U_f} = \frac{1}{U_{cl}} + R_{f,tot}$
Heat duty (kW)	$\dot{Q} = U \times A_e \times \Delta T_{LMTD}$

**Table A-2**

Constants used in the gasketed PHXs for single-phase heat transfer and pressure drop measurement.

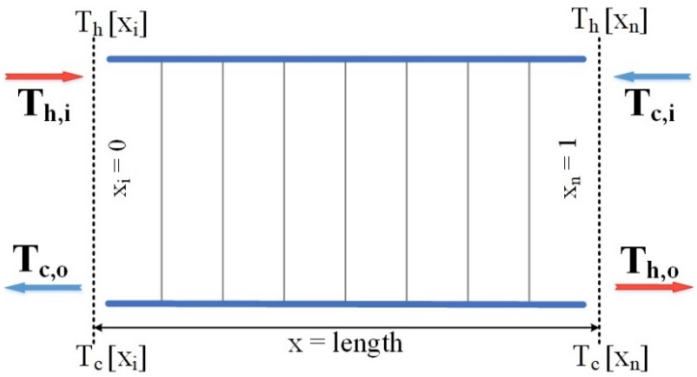
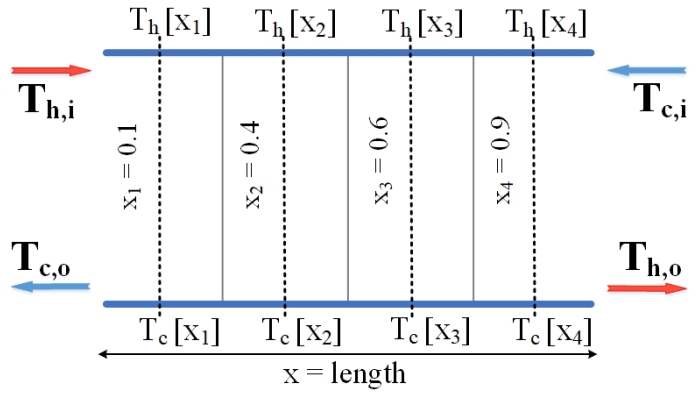
Chevron angle (degree)	Thermal			Hydraulic		
	Re	C <sub>h</sub>	$n'$	Re	K <sub>P</sub>	m
≤ 30	≤10	0.718	0.349	<10	50.000	1.000
	>10	0.348	0.663	10–100	19.400	0.589
				>100	2.990	0.183
45	<10	0.718	0.349	<15	47.000	1.000
	10–100	0.400	0.598	15–300	18.290	0.652
	>100	0.300	0.663	>300	1.441	0.206
50	<20	0.630	0.333	<20	34.000	1.000
	20–300	0.291	0.591	20–300	11.250	0.631
	>300	0.130	0.732	>300	0.772	0.161
60	<20	0.562	0.326	<40	24.000	1.000
	20–400	0.306	0.529	40–400	3.240	0.457
	>400	0.108	0.703	>400	0.760	0.215
≥ 65	<20	0.562	0.326	50	24.000	1.000
	20–500	0.331	0.503	50–500	2.800	0.451
	>500	0.087	0.718	>500	0.639	0.213

**Table 1.**

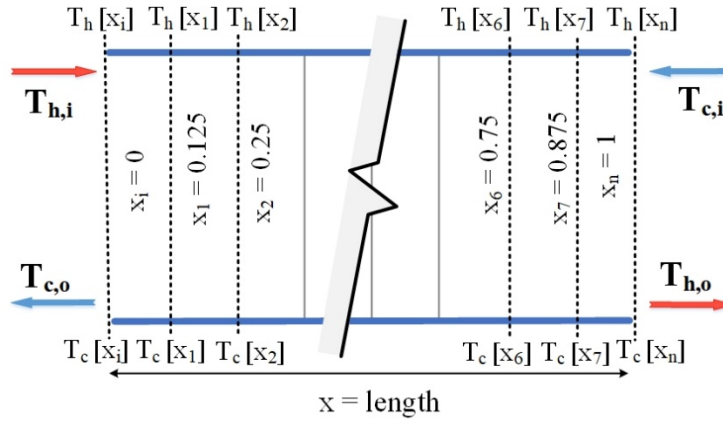
Geometric conditions of an experimental and actual industrial-scale heat exchanger.

Parameter	Value	
	Experimental	Industrial [35]
<b><u>Process</u></b>		
Mass flow rate (hot/cold), $kg/s$	0.01871/0.01697	50/50
Inlet temperature (hot/cold), $^{\circ}C$	53.04/40.34	65/22
outlet temperature (hot/cold), $^{\circ}C$	44.84/47.4	45/42
<b><u>Geometric</u></b>		
Plate thickness, $t$ , mm	0.6	0.6
Chevron angle, $\beta$	$60^{\circ}$	$30^{\circ}$ - $65^{\circ}$
Total plates	20	35
Enlargement factor, $\phi$	1.15	1.25
Total passes (cold/hot)	1/1	1/1
Effective area, $A_e, m^2$	0.432	35.08
Diameter of all port, $D_p$ , mm	24	200
Compressed length of plate pack, $L_c$ , mm	65	380
Distance of vertical port, $L_v$ , mm	243	1550
Distance of horizontal port, $L_h$ , mm	72	430
Width of effective channel, $L_w$ , mm	96	630
Plate thermal conductivity, $k'$ , W/m.K	17.5	20
Plate material	SS	SS

**Table 2.**  
Numerical approaches details.

Approach	Graphic description	Mathematical formulation
Arithmetic mean		$k = 2, x = 0, 1$ $U = \int_{T_{h,i}}^{T_{h,o}} \frac{-\dot{C}_h dT_h}{A \Delta T} \approx \frac{\dot{m}_h (T_{h,o} - T_{h,i})}{2} \left[ \left( \frac{c_{p,h}}{A \Delta T} \right)_0 + \left( \frac{c_{p,h}}{A \Delta T} \right)_1 \right]$ $T_{h[0]} = T_{h,i}$ $T_{h[1]} = T_{h,i} - \Delta T_h$ $\Delta T_h = T_{h,i} - T_{h,o}$
Chebyshev integration		$k = 4, x = 0.10, 0.40, 0.60, 0.90$ $U = \int_{T_{h,i}}^{T_{h,o}} \frac{-\dot{C}_h dT_h}{A \Delta T} \approx \frac{\dot{m}_h (T_{h,o} - T_{h,i})}{4} \left[ \left( \frac{c_{p,h}}{A \Delta T} \right)_{0.10} + \left( \frac{c_{p,h}}{A \Delta T} \right)_{0.40} \dots \right. \\ \left. + \left( \frac{c_{p,h}}{A \Delta T} \right)_{0.90} \right]$ $T_{h[0.10]} = T_{h,i} - 0.10 \Delta T_h$ $\vdots$ $T_{h[0.90]} = T_{h,i} - 0.90 \Delta T_h$

Simpsons  
(n = 2,4,8)



$$\Delta x = \frac{x_n - x_i}{n} \quad \therefore n = 2, 4 \text{ and } 8$$

$$x_i = 0, x_1 = x_i + \Delta x, x_2 = x_1 + \Delta x \dots, x_n = 1$$

For simpson n = 8,

$$k = 9, \Delta x = 0.125, x = 0, 0.125, 0.25 \dots 0.875, 1$$

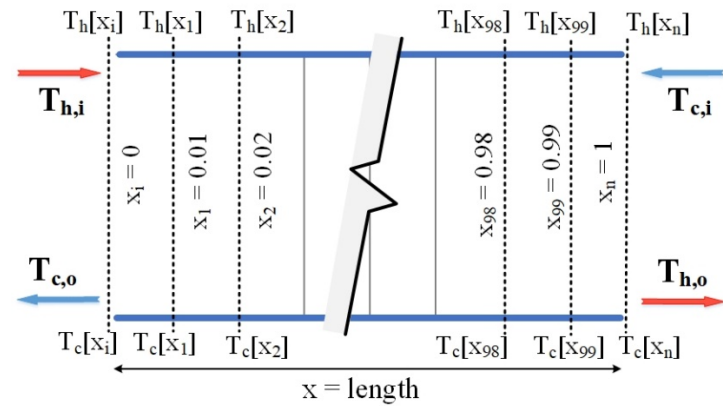
$$U = \int_{T_{h,i}}^{T_{h,o}} \frac{-\dot{C}_h dT_h}{A \Delta T} \approx \frac{\dot{m}_h (T_{h,o} - T_{h,i})}{9} \left[ \left( \frac{c_{p,h}}{A \Delta T} \right)_0 + \left( \frac{c_{p,h}}{A \Delta T} \right)_{0.125} \dots + \left( \frac{c_{p,h}}{A \Delta T} \right)_1 \right]$$

$$T_{h[0]} = T_{h,i}; \quad T_{h[0.125]} = T_{h,i} - 0.125 \Delta T_h$$

⋮

$$T_{h[1]} = T_{h,i} - \Delta T_h$$

Exact  
Numerical  
(n=100)



$$k = 101, x = 0, 0.01, 0.02 \dots 0.99, 1$$

$$U = \int_{T_{h,i}}^{T_{h,o}} \frac{-\dot{C}_h dT_h}{A \Delta T} \approx \frac{\dot{m}_h (T_{h,o} - T_{h,i})}{101} \left[ \left( \frac{c_{p,h}}{A \Delta T} \right)_0 + \left( \frac{c_{p,h}}{A \Delta T} \right)_{0.01} \dots + \left( \frac{c_{p,h}}{A \Delta T} \right)_1 \right]$$

$$T_{h[0]} = T_{h,i}; \quad T_{h[0.01]} = T_{h,i} - 0.01 \Delta T_h$$

⋮

$$T_{h[1]} = T_{h,i} - \Delta T_h$$

**Table 3.**  
Experimental data.

Data set	Process parameters		
	$T_{c,i}/T_{c,o}$ (°C)	$T_{h,i}/T_{h,o}$ (°C)	$V_c/V_h$ (l/min)
Run 1	20/33	47/31	1.03/0.92
Run 2	33/44	50/45	0.97/2.08
Run 3	20/34	48/33	1.75/1.65
Run 4	20/34	47/33	1.75/1.76
Run 5	25/33	45/34	1.95/1.86
Run 6	26/38	49/39	1.94/2.35
Run 7	32/37	50/38	2.27/2.12
Run 8	27/32	48/31	3.71/1.35
Run 9	27/30	47/32	3.19/2.13
Run 10	27/32	48/33	3.69/2.10

**Table 4.**

Comparison of the averaging method for industrial-scale PHX.

<b>Method</b>	<b>A (m<sup>2</sup>)</b>	$(A_{approach} - A_{const})$ $/ A_{const} \times 100$
Constant	35.08	0
Arithmetic mean	40.43	+15.25
Chebyshev	40.25	+14.74
Simpson (n = 2)	40.34	+14.99
Simpson (n = 4)	40.3	+14.88
Simpson (n = 8)	40.27	+14.79
Exact (n = 100)	40.26	+14.76

## List of Figure Captions

**Figure 1.** Experimental arrangement, (a) actual system, and (b) schematic illustration.

**Figure 2.** Chevron plate characteristics.

**Figure 3.** Numerical analysis flow chart.

**Figure 4.** Validation with laboratory-scale PHX.

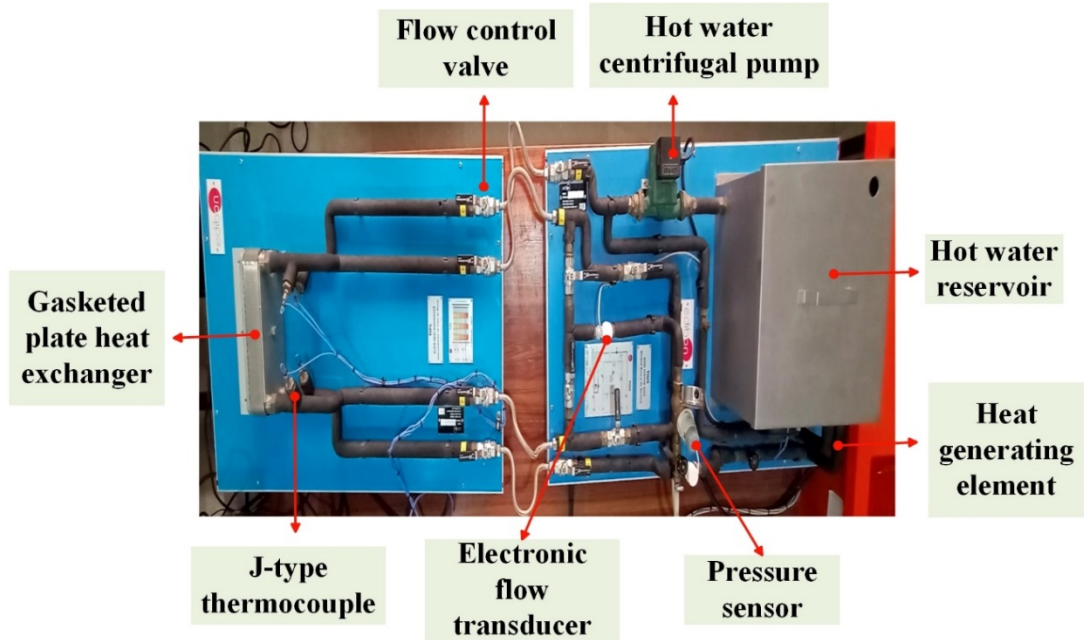
**Figure 5.** Variation in  $h$  for laboratory-scale PHX by (a) Arithmetic mean (b) Chebyshev method (c) Simpson ( $n=2$ ) method, (d) Simpson ( $n=4$ ) method, (e) Simpson ( $n=8$ ) method, and (f) Exact numerical ( $n=100$ ).

**Figure 6.** Heat transfer coefficient for industrial-scale HX at a different angle by (a) Arithmetic mean method (b) Chebyshev method (c) Simpson ( $n=2$ ) method (d) Simpson ( $n = 4$ ) method (e) Simpson ( $n = 8$ ) method (f) Exact ( $n = 100$ )

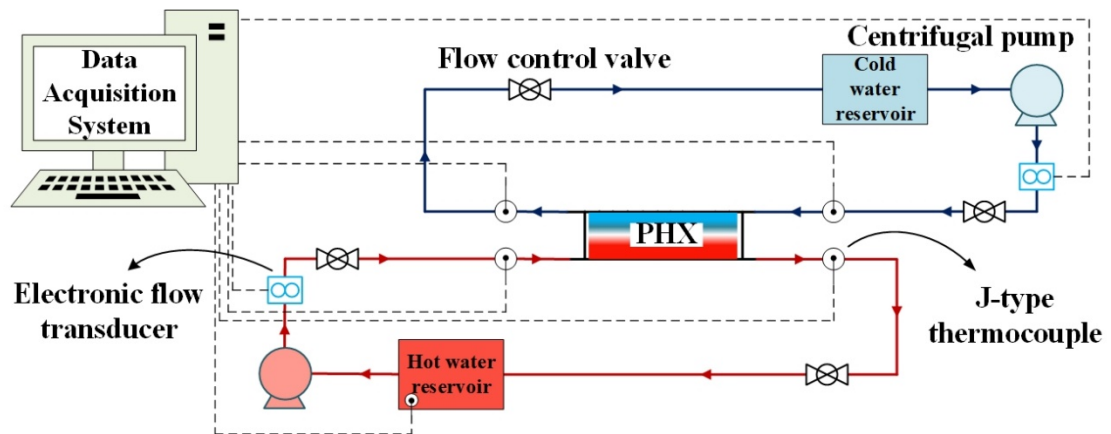
**Figure 7.** Heat Transfer coefficient for different fluid.



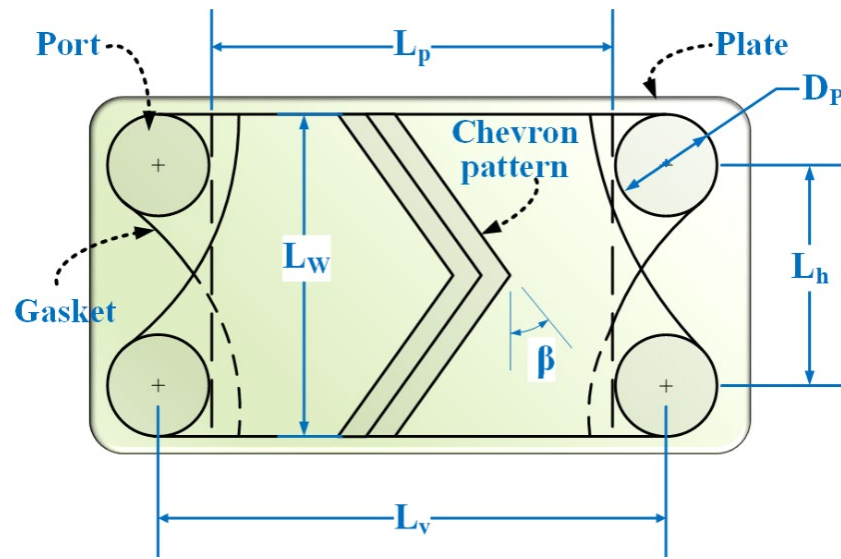
(a)



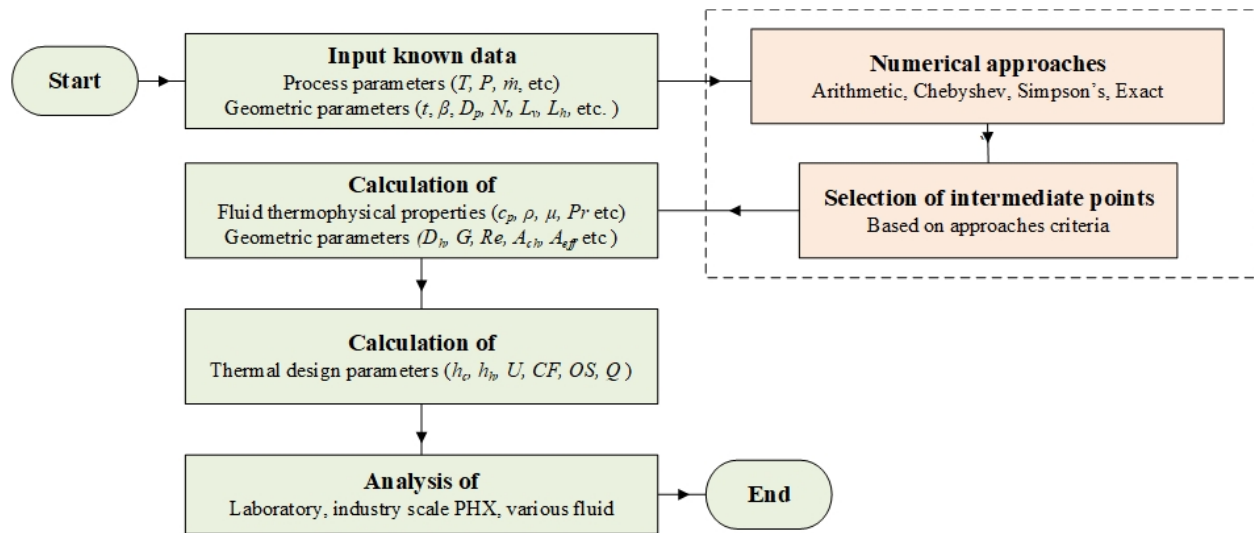
(b)



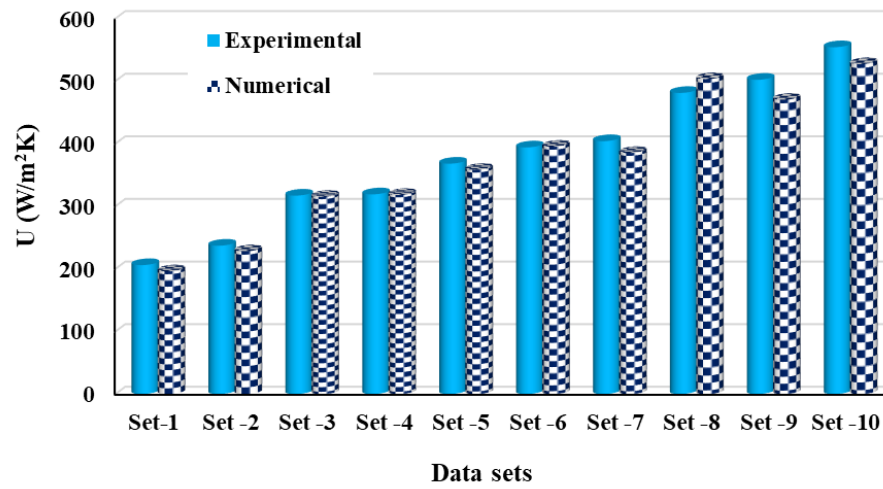
**Figure 1.** Experimental arrangement, (a) actual system, and (b) schematic illustration.



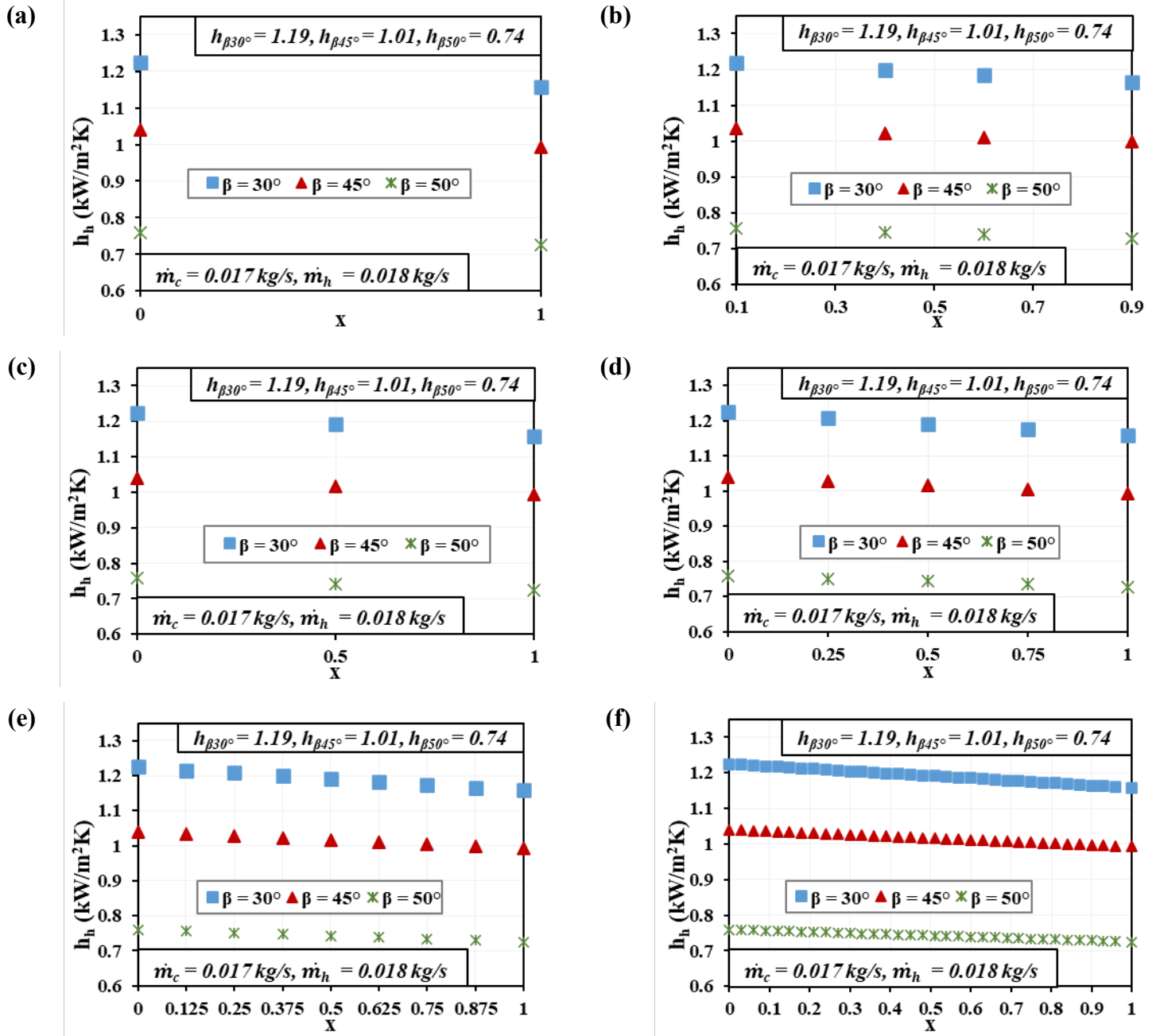
**Figure 2.** Chevron plate characteristics.



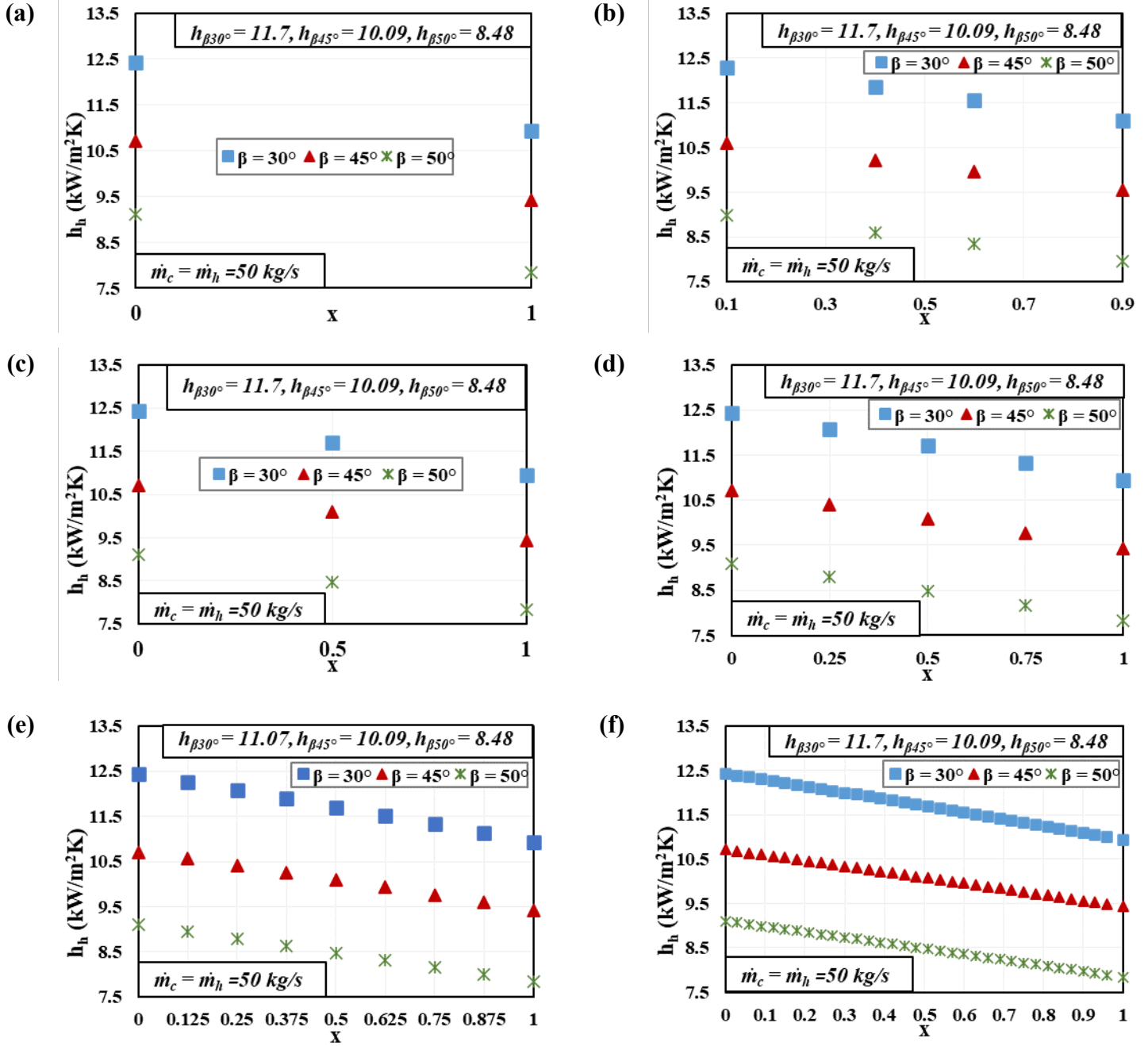
**Figure 3.** Numerical analysis flow chart.



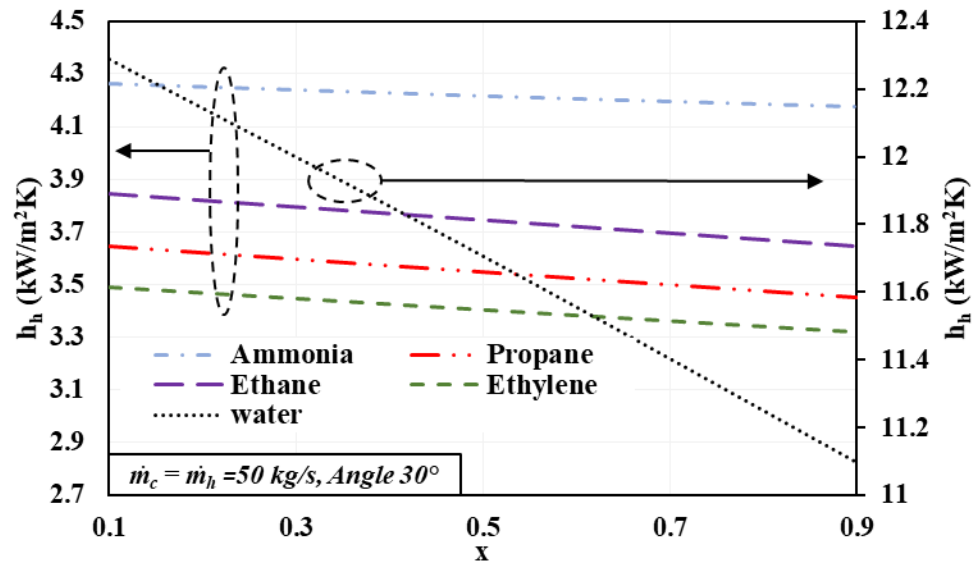
**Figure 4.** Validation with laboratory-scale PHX.



**Figure 5.** Variation in  $h$  for laboratory-scale PHX by (a) Arithmetic mean (b) Chebyshev method (c) Simpson (n=2) method, (d) Simpson (n=4) method, (e) Simpson (n=8) method, and (f) Exact numerical (n=100).






**Figure 6.** Heat transfer coefficient for industrial-scale HX at a different angle by (a) Arithmetic mean method (b) Chebyshev method (c) Simpson (n=2) method (d) Simpson (n = 4) method (e) Simpson (n = 8) method (f) Exact (n = 100)




**Figure 7.** Heat Transfer coefficient for different fluid.

## Notes on contributors

	<p><b>Muhammad Ahmad Jamil</b> is doing PhD from Mechanical and Construction Engineering Department, Northumbria University, Newcastle Upon Tyne UK. He earned his master's degree in Mechanical Engineering from King Fahd University of Petroleum and Minerals, Dhahran, Saudi Arabia, in 2017. He has worked as co-PI in various funded projects at the national and international levels. Currently, he is working in the fields of cooling, heat transfer, and clean water. <b>He has published 20 peer-reviewed journal papers.</b></p>
	<p><b>Talha S. Goraya</b> is currently a bachelor student of mechanical engineering at Khwaja Fareed University of Engineering and Information Technology (KFUEIT), Rahim-Yar-Khan, Pakistan. He is working on heat exchanger analysis and optimization. He has Published 04 peer-reviewed journals papers.</p>
	<p><b>Haseeb Yaqoob</b> is working as a Lecturer at the Department of Mechanical Engineering at Khwaja Fareed University of Engineering and Information Technology (KFUEIT), Rahim-Yar-Khan, Pakistan. Currently, he is teaching and conducting research in the fields of heat transfer, renewable energy, and alternative fuels.</p>
	<p><b>Muhammad Wakil Shahzad</b> is working as Senior Lecturer in Mechanical and Construction Engineering Department at Northumbria University, Newcastle Upon Tyne, UK. His research is focused on water treatment, hybrid desalination processes (MEDAD), renewables, and their integration for green and sustainable water production. His hybrid MEDAD cycle is successfully commercialized in Saudi Arabia. He developed solar thermal energy storage batteries for building heating network decarbonization. He is working on commercial buildings and data center cooling using non-conventional air-conditioning technology. He is a member of two spin-off companies: MEDAD technologies for water treatment system commercialization and K-COOL for cooling cycle commercialization. He holds 8 international patents published 2</p>



	book, 17 book chapters, 60 peer-reviewed journal papers and over 100 conference papers.
	<p><b>Syed M. Zubair</b> is a Distinguished Professor in the Department of Mechanical Engineering at KFUPM, Dhahran, Saudi Arabia. He earned his Ph.D. in Mechanical Engineering from Georgia Institute of Technology, Atlanta. His research interest involves both applied as well as fundamental areas of energy and desalination systems, refrigeration and air-conditioning systems, and fouling of heat exchangers. He has participated in several research projects, including projects supported by MIT-KFUPM Center for Clean Water and Clean Energy. The heating and dehumidification (HDH) technology he developed with MIT collaborators ended up in a commercial application to treat produced water from oil and gas wells. He has published over 250 research papers and was awarded 8 US patents. Currently, he is serving on the editorial board of the International Journal of Refrigeration and as Associate Editor of Nature Partner Journal (npj) Clean Water.</p>